Unusual Polystyrene Nanocomposite Structure Using Emulsifier-Modified Layered Double Hydroxide as Nanofiller

Abdallah Illaik,[†] Christine Taviot-Guého,[†] Jérôme Lavis,[‡,§] Sophie Commereuc,[||,⊥] Vincent Verney,[||] and Fabrice Leroux*,[†]

Laboratoire des Matériaux Inorganiques, UMR CNRS-UBP 6002, Université Blaise Pascal (Clermont-Ferrand), 24 av. des Landais, 63177 Aubière cedex, France, Chimie Moléculaire et Organisation du Solide, UMR 5637, Université Montpellier II, CC 007, place Eugène Bataillon, 34095 Montpellier cedex 05, France, Laboratoire de Photochimie Moléculaire et Macromoléculaire, UMR CNRS-UBP 6505, Université Blaise Pascal (Clermont-Ferrand), 24 av. des Landais, 63177 Aubière cedex, France, and Ecole Nationale Supérieure de Chimie de Clermont-Ferrand (ENSCCF), Campus des Cézeaux, 63174 Aubière cedex, France

Received January 22, 2008. Revised Manuscript Received April 8, 2008

A new hybrid organic inorganic assembly between an emulsifier, 4[12-(methacryloylamino)dodecanoylamino] benzenesulfonate acid (MADABS) and layered double hydroxide (LDH) of cation composition Zn_2Al is described, as well as its subsequent dispersion into styrene. The characterization of the new hybrid LDH assembly by 1D electron density pictures the interleaved emulsifier well ensconced between LDH sheets, while showing the impossibility for the molecules to polymerize themselves. Indeed, the strong interdigitation abates the in situ polymerization. LDH/emulsifier:polystyrene nanocomposites, Zn_2Al/MADABS:PS, are prepared by bulk polymerization, and "apparent immiscible" and intercalated PS nanocomposite structures are alternatively observed as a function of the thermal pretreatment of the filler. The rheological data are indicative of microstructural changes between the samples. For the precalcined filler, the PS nanocomposite presents a shear thinning exponent of -0.55 in the low frequency domain, associated to a hump shape for the damping coefficient δ, both curvatures consistent with the increase of glass transition temperature T_g, whereas the other sample exhibits a shear thinning exponent of 0 and a general behavior closely related to PS in spite of an increase in the elastic modulus G' and the loss modulus G'' of small amplitude. Such differences in the nanocomposite structure are further confirmed by TEM direct observations, with the presence of a tactoid network or of particle agglomerates when the filler is precalcined or not, respectively. Contrary to the general idea that pervades that intercalated polymer structure means an increase in the interaction between polymer chain and filler and consequently an enhancement of the mechanical properties, it is here demonstrated that such a behavior may be in conjunction with agglomerates while an opposite tendency is observed for the non-intercalated structure with the observation of an unusual solid-like structure for PS nanocomposite arising from friction welding effects between LDH tethered MADABS molecules and PS polymer chains.

1. Introduction

Since the pioneering work of Toyota's R&D in the 1990s,[1–3] research on polymer nanocomposites has been boosted in the last 15 years and is still the subject of growing interest because high-performance nanocomposites are needed in different applications such as those emphasizing mechanical enhancement, gas permeability, fire retardancy, or polymer electrolyte.[4–8] Mostly dealing with smectite-type materials, recent works consider layered double hydroxides (LDH) as inorganic nanofillers. Indeed, LDH materials are presenting advantages in comparison to smectites such as montmorillonite due to both its versatility in chemical composition and tunable charge density, allowing multiple interactions with the polymer.[9–11]

Hydrotalcite-like compounds, hereafter called LDH-type materials, are described according to the ideal formula, $[M^{II}_{1-x}M^{III}_x(OH)_2]^{x+}_{intra}[A^{m-}_{x/m}\cdot nH_2O]_{inter}$, where M^{II} and M^{III} are metallic cations, A the anions, and *intra* and *inter* denote the intralayer and interlayer domain, respectively. The

* Corresponding author. E-mail: fabrice.leroux@univ-bpclermont.fr.
[†] Laboratoire des Matériaux Inorganiques, Université Blaise Pascal.
[‡] Université Montpellier II.
[§] Present address: Chemistry Department, 364 The Seymour and Esther Padnos Hall of Science, Grand Valley State University, Allendale, Michigan 49401-9403.
[||] Laboratoire de Photochimie Moléculaire et Macromoléculaire, Université Blaise Pascal.
[⊥] Ecole Nationale Supérieure de Chimie de Clermont-Ferrand.

(1) Usuki, A.; Kojima, Y.; Kawasumi, M.; Okada, A.; Fukushima, Y.; Kuruachi, T.; Kamigaito, O. *J. Mater. Res.* **1993**, *8*, 1179.
(2) Kamigaito, O.; Kawasumi, M.; Hohzaki, M.; Kojima, Y.; Okada, A. U.S. Patent 4810743, 1993.
(3) Yano, K.; Usuki, A.; Okada, A.; Kurauchi, T.; Kamigaito, O. *J. Polym. Sci., Part A* **1993**, *31*, 2493.
(4) Giannelis, E. P.; Krishnamoorti, R.; Manias, E. *Adv. Polym. Sci.* **1999**, *38*, 107.
(5) Alexandre, M.; Dubois, P. *Mater. Sci. Eng.* **2000**, *28*, 1.
(6) Ray, S. S.; Okamoto, M. *Prog. Polym. Sci.* **2003**, *28*, 1539.
(7) Utracki, L. A.; Sepehr, M.; Boccaleri, E. *Polym. Adv. Technol.* **2007**, *18*, 1.
(8) Liff, S. M.; Kumar, N.; McKinley, G. H. *Nat. Mater.* **2007**, *6*, 76.
(9) Ding, P.; Chen, W.; Qu, B. *Prog. Nat. Sci.* **2006**, *16*, 573.
(10) Evans, D. G.; Duan, X. *Chem. Commun.* **2006**, 485.
(11) Leroux, F. *J. Nanosci. Nanotechnol.* **2006**, *6*, 303.

10.1021/cm800212g CCC: $40.75
Published on Web 07/15/2008

structure consists of brucite-like layers constituted of edge-sharing octahedra. The presence of trivalent cations induces positive charges in the layers which are counterbalanced by interlamellar anions. Their exchange capacity makes LDH structure a promising host for a large number of applications;[12–15] furthermore, LDH materials can be considered as filler for polymer owing to their structural anisotropy.

It is generally accepted that the use of layered crystalline materials as nanofiller is conditioned upon their ability to undergo intercalation or exfoliation by polymer chains, even though exfoliation versus intercalation nanocomposite structure has always been a great issue. Yet, no satisfactory explanation has been provided that ascertains the desirability of a complete exfoliation toward the enhancement of the properties of the nanocomposite. It has been demonstrated lately that the morphology of the nanocomposite may be substantially more complex than initially envisioned.[16] Although beneficial to the increase of tortuosity and therefore the decrease of permeation, the exfoliation of inorganic platelets is not an absolute prerequisite in the case of fire retardant nanocomposites. Yet, its effect on the mechanical properties is questionable[17] since the intercalated nanocomposite structure may provide "nanosprings" helpful for releasing applied stress. Indeed, a strong adhesion between the polymer parts and the filler may play a key role in transferring stress from the low-modulus polymer to the high-modulus mineral filler. It may come from a filler intimately mixed into the polymer (i.e., exfoliation for a 2D-type filler) or from a strong interaction between the two components (i.e., incorporation of chains, covalent bonding). Additionally, to render the inorganic platelets organophilic, long chain organic molecules are often needed. This presents the advantage of propping apart the lamellae, thus helping the exfoliation process without the need for any pretreatment. However, an alternative and enticing approach is to use reactive organophilic fillers in order to achieve strong interactions between the two components of the nanocomposite. This is inspired by the chemistry involved in thermoset polymers such as epoxide, and has been recently used to produce chemical linkages between polymer and filler by incorporating either a coupling agent[18] or a monomer surfactant.[19,20] In the latter case, the styryl monomer on the ammonium montmorillonite compatibilizing molecule was found to participate in the polymerization reaction but not sufficient to induce exfoliation.

The use of surfactant monomer adapted to LDH-type filler is scarce, and one may find it difficult to discern a general trend. Using polymethylmethacrylate (PMMA) and different polymerizable molecules incorporated into LDH filler, PMMA structure varies from micrometer-sizes agglomerates of LDH particles clustering together[21] to exfoliated systems.[22,23] A longer carbon backbone, such as 10-undecenoate, seems to favor the miscibility between LDH platelets and the polymer. In some cases, the preparation process may deteriorate the lamellar LDH structure, leading to decomposition.[24]

Scheme 1. Representation of MADABS[a]

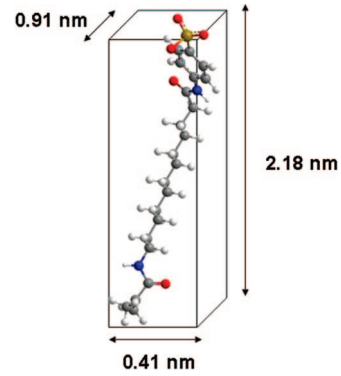

[a] Atom color code: grey, carbon; white, hydrogen; yellow, sulphur; red, oxygen; blue, nitrogen.

The objective of this research was to prepare a new organic−inorganic LDH assembly using a long alkyl chain monomer as interleaved molecule and to study the behavior of the resulting sandwiched organic−inorganic heterostructure as filler for polymer. We choose 4-[12-(methacryloylamino)dodecanoylamino] benzenesulfonate acid (abbreviated hereafter as MADABS and described in Scheme 1) as compatibilizer to lipophilize the surface of the inorganic platelets with also the possibility through its acryloyl function to polymerize during bulk polymerization.

2. Experimental Section

Synthesis. 4-[12-(Methacryloylamino)dodecanoylamino]benzenesulfonate acid abbreviated MADABS ($H_2C{=}C(CH_3){-}CO{-}NH{-}(-CH_2-)_{11}{-}CO{-}NH{-}C_6H_4{-}SO_3H$, M_w = 438 g·mol^{-1}) was prepared according to De Winter et al.[25] This protocol is summarized as follows: laurinlactam was stirred in aqueous NaOH at 220 °C for 8 h. It was then treated in H_3PO_4 at 90 °C for 30 min and recrystallized in 60% aqueous THF to give 12-aminododecanoic acid. The product was then refluxed for 1 h in acetone with methacryloyl chloride with $NaHCO_3$ and *p*-methoxyphenol. The mixture was poored on water, filtered and recrystallized from ethyl acetate to give 12-(methacryloylamino)dodecanoic acid. This product was reacted with thionyl chloride in DMF at room temperature for 2 h. The reaction mixture was added dropwise at room temperature to a solution of sulfanilic acid and pyridine in DMF. The final product was recovered after filtration and washing with KOH in methanol. It was recrystallized in a water/methanol (20/80) mixture to give 4-[12-(methacryloylamino)dodecanoylamino]benzenesulfonate (MADABS) acid. $ZnCl_2$, $Al(NO_3)_3 \cdot 9H_2O$ (Acros, 99%), NaOH (Acros, 97%), benzoyl peroxide (BPO,

(12) Leroux, F.; Besse, J.-P. *Chem. Mater.* **2001**, *13*, 3507.
(13) Hibino, T. *Encycl. Nanosci. Nanotechnol.* **2004**, *7*, 657.
(14) Leroux, F.; Taviot-Guého, C. *J. Mater. Chem.* **2005**, *15*, 3628.
(15) Choy, J.-H.; Park, M.; Oh, J.-M. *Curr. Nanosci.* **2006**, *2*, 275.
(16) Schaefer, D. W.; Justice, R. S. *Macromolecules* **2007**, *40*, 8501.
(17) Strawhecker, K. E.; Manias, E. *Chem. Mater.* **2000**, *12*, 2943.
(18) Xu, M.; Zhang, T.; Gu, B.; Wu, J.; Chen, Q. *Macromolecules* **2006**, *39*, 3540.
(19) Wang, D.; Zhu, J.; Yao, Q.; Wilkie, C. A. *Chem. Mater.* **2002**, *14*, 3837.
(20) Su, S.; Wilkie, C. A. *J. Polym. Sci., Part A* **2003**, *41*, 1124.
(21) Costache, M. C.; Wang, D.; Heidecker, M. J.; Manias, E.; Wilkie, C. A. *Polym. Adv. Technol.* **2006**, *17*, 272.
(22) Wang, G.-A.; Wang, C.-C.; Chen, C.-Y. *Polymer* **2005**, *46*, 5065.
(23) Wang, G.-A.; Wang, C.-C.; Chen, C.-Y. *J. Inorg. Organomet. Polym. Mater.* **2005**, *15*, 239.
(24) Ding, P.; Qu, B. *J. Appl. Polym. Sci.* **2006**, *101*, 3758.
(25) de Winter, X.; Mariën, A.; Michiels, E. *Bull. Soc. Chim. Belg.* **1990**, *99*, 977.

Aldrich, 97%), and styrene in presence of an inhibitor (1,2 dihydroxy 4-*tert*-butylbenzene) were used as received, except for the monomer which was purified by distillation under reduced pressure at 50 °C.

Preparation of the LDH Hybrid Materials. The cation LDH composition of the LDH material was Zn_2Al, and the preparation of the hydrotalcite-like hybrid materials was performed using the so-called coprecipitation method. Experimentally, a solution of MADABS (4×10^{-2} M) was prepared, and 250 mL of solution of the salts (Zn; 2×10^{-2} M and Al; 1×10^{-2} M) were added dropwise to the previous solution. During the addition, the reaction was kept under nitrogen atmosphere to avoid contamination by carbonate, and the pH was kept constant at 10.0 ± 0.1 with the addition of NaOH. The slurry was aged in the mother liquid and separated by centrifugation. The resulting powders hereafter named as Zn_2Al/MADABS were washed several times with distilled water and finally dried at room temperature.

Elemental analysis (N, S, Al, and Zn) was performed at the Vernaison Analysis Center of CNRS using inductive conduction plasma coupled to atomic emission spectroscopy (ICP/AES). The chemical composition reported from elemental analyses was Zn, 15.89; Al, 3.29; N, 3.34; S 3.81% and from the water molecule content calculated from the weight loss under air was $Zn_2Al(OH)_6(MADABS)_{0.98}(CO_3^{2-})_{0.01}\cdot 7.41H_2O$ (M_w = 822.1 g·mol^{-1}) for Zn_2Al/MADABS. The final weight loss was in agreement with the complete combustion of the organic molecule and the formation of the composition "$Zn_2AlO_{7/2}$"; TG analysis is supplied in Supporting Information (SEI-1).

Preparation of the Nanocomposites. The nanocomposites were prepared by bulk polymerization using BPO as initiator. Bulk polymerization was preferred to polymer melt because the process may involve more interactions by tethering the platelets surface to the polymer chains. The dispersion used here was not sophisticated, and no special care was taken in terms of grinding. Room temperature LDH phase Zn_2Al/MADABS or calcined at 200 °C and BPO (0.1 wt %) were incorporated into 5 mL of a distilled solution of styrene. A filler loading of 10% of the total mass was incorporated into styrene; PS:hybrid filler = 90:10) (wt %). Strictly speaking, this corresponds to a percentage of inorganic filler "$Zn_2Al(OH)_6$" of roughly 3.6 wt %. The mixture was vigorously stirred for 4 h at room temperature, sonicated for 15 min, and then placed for 1 h under nitrogen atmosphere before the polymerization. At this step, cloudy suspensions were found to be stable in styrene for a long time. The polymerization process was induced by heat at 80 °C for 24 h for styrene (free of filler), whereas a temperature of 95 °C was needed for the nanocomposites to complete the polymerization. Remaining styrene was removed from the nanocomposites by a thermal treatment at 60 °C under vacuum.

Characterization. XRD analyses of the hybrid LDH and polymer nanocomposites were performed on a Siemens D501 diffractometer using a Cu Kα source; data were collected in a step scan mode between 2.0 and 70.0° (2θ), with a step size of 0.03° (2θ) and a counting time of 10 s/step.

One-dimensional (1D) electron density calculations based on X-ray diffraction are often carried out to probe the structure of the incorporated species in two-dimensional inorganic hosts.[26–28] This yields specific information about the orientation and structure of the incorporated species or at least eliminates certain conformational possibilities, which are incompatible with the diffraction data. The electron density maps were obtained from eq 1:

$$\rho(z) = \sum_{l=0}^{\infty} F_{00l} \cos\left(\frac{2\pi l z}{c}\right) \quad (1)$$

The structure factors of the 00*l* reflections F_{00l} were derived from their intensities corrected for Lorentz polarization effects. The signs of the structure factors were directly obtained from the scattering contributions of Zn_2Al hydroxide layers assuming that the contribution of incorporated molecule is relatively small. c is the unit cell parameter. Six 00*l* reflections were used for Zn_2Al/MADABS.

Transmission electron microscopy images were taken on a Hitachi H-7650 operating at 80 kV, from ultrathin cuts deposited on copper grid coated with a carbon layer.

Size exclusion chromatography (SEC) measurements were carried out with a Viscotek Trisec 270 Controller as a viscosimetric detector and a VE3580 Viscotek refractive index detector. The mobile phase was THF (Aldrich HPLC grade) with a flow rate of 1 mL/min, and separation was achieved using a GMHxl column. The calibration curve was obtained using polystyrene standards. Average molecular weights (M_w and M_n) were calculated, as well as the polydispersity index ($I_p = M_w/M_n$). Experimentally, filler-free polymers were solubilized in THF and then directly injected, whereas prior to injection, the polymers obtained from the as-made nanocomposites were obtained after a first dissolution in THF and then filtration and recrystallization in ethanol. For PS: M_w = 191 000 g·mol^{-1}, $I_p = 3.5$. For Zn_2Al/MADABS:PS M_w = 158 000 g·mol^{-1}, $I_p = 3.03$. For Zn_2Al/MADABS-T:PS, M_w = 175 000 g·mol^{-1}, $I_p = 3.3$.

The melt rheological properties of the polymer nanocomposite were measured at different temperatures (180, 200, 220, and 240 °C) using a spectrometer StressTECh Rheologica with a parallel plate geometry (plate diameter 10 mm, gap 1 mm) in oscillatory mode, and linear viscoelastic properties were studied under dynamic oscillatory shearing using the input strain function $\gamma(t) = \gamma_0 \sin(\omega t)$, with frequency ranging from 0.003 to 30 Hz (≈0.02 to 200 rad/s). The imposed oscillatory shear stress amplitude was tested for each temperature to validate the measurements inside the linear viscoelastic domain.

3. Results and Discussion

3.1. Zn_2Al/MADABS Inorganic/Organic (I/O) Hybrid Phase. The Zn_2Al/MADABS hybrid phase was obtained by coprecipitation as a pure phase, and the chemical composition is consistent with what is expected for a complete precipitation of the metal salts (see Experimental Section). After calcinations in air at 200 °C, the material was designed as Zn_2Al/MADABS-200.

The X-ray powder diffraction pattern of Zn_2Al/MADABS is shown in Figure 1. A broad diffraction pattern is observed indicating a poor crystallinity likely due to small particle size and microstrain effects related to the size of the large incorporated molecule. Yet, the relatively large number of 00*l* reflections observed, up to 11 harmonics, indicates a rather ordered interlayer organization. Besides, the broad hump centered at approximately 21° (2θ) is characteristic of long alkyl-chain incorporated phases as previously observed in the case of dodecylbenzene sulfonate containing

(26) Bauer, J.; Behrens, P.; Speckbacher, M.; Langhals, H. *Adv. Funct. Mater.* **2003**, *13*, 241.
(27) Itoh, T.; Shichi, T.; Yui, T.; Takahashi, H.; Inui, Y.; Takagi, K. *J. Phys. Chem. B* **2005**, *109*, 3199.
(28) Whittingham, M. S.; Jacobson, A. J. *Intercalation Chemistry*; Academic Press: New York, 1982.

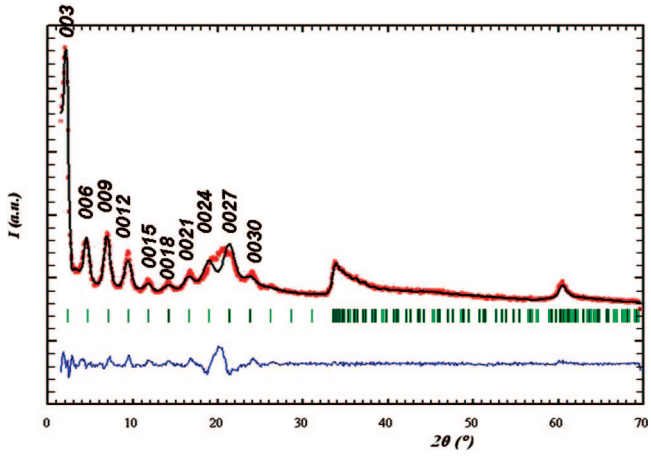

Figure 1. Profile matching of the powder X-ray diffraction pattern of Zn_2Al/MADABS in the 2θ range 2−70°: experimental X-ray diffraction (dot), calculated (line), Bragg reflections (ticks, and difference profile.

LDH.[29,30] The diffraction peaks were indexed based on a hexagonal unit cell with the space group $R\bar{3}m$, generally admitted in the LDH system. The first diffraction peak at low 2θ angle corresponds to the 003 Bragg reflections and gives access to the interlayer distance $d_{003} \sim 3.75$ nm. If one assumes a thickness of approximately 0.48 nm for the hydroxide layer,[31] the available height for the incorporated MADABS molecule is ∼3.27 nm. A profile refinement of the powder X-ray diffraction diagram was attempted leading to the following cell parameters: $a = 0.3074(1)$ nm and $c = 11.24(1)$ nm, that is, $3d_{003}$. The value of the a parameter is in agreement with a metallic ratio $R = Zn/Al$ equal to 2 within the hydroxide layers displaying 0.248 nm^2 available surface area per charge. On the other hand, the dimensions of the MADABS molecule were obtained from steric energy minimization using the MM2 method.[32] MADABS has an approximate parallelepiped shape of 2.180.41 × 0.91 nm (Scheme 1). Thus, the observed interlayer distance must arise from a head-to-tail bilayer packing arrangement of MADABS molecules with the sulfonate groups interacting with the hydroxylated sheets. In such an orientation, the MADABS requires a surface area of ∼0.157 nm^2 per unit charge largely satisfied by the host lattice (0.248 nm^2/e^-). Either a perpendicular or a tilted arrangement could be envisaged with different degrees of interdigitation. To get further insight into the interlayer arrangement of MADABS molecules, the 1D electron density map, $\rho(Z)$, of Zn_2Al/MADABS structure along the c axis was constructed (Figure 2). $\rho(Z)$ values were obtained by a Fourier transform of the 006/009/0012/0015/0018/0021 reflection intensities. The 1D electron density map displays two strong peaks at $d = 0$ and 3.75 nm due to the hydroxide layers. Six additional peaks of lower electron density arising from the interlayer content are observed: the sulfonate groups cause maxima at the outer parts of the interlayer space, that is, $d \sim 0.59$ and 3.15 nm; the four central maxima spaced approximately 5.1 Å from each other are attributed to the alkyl chain. Upon comparison with the length of the MADABS molecule, an interdigitated bilayer arrangement with a tilt angle of ∼20−25° is proposed.

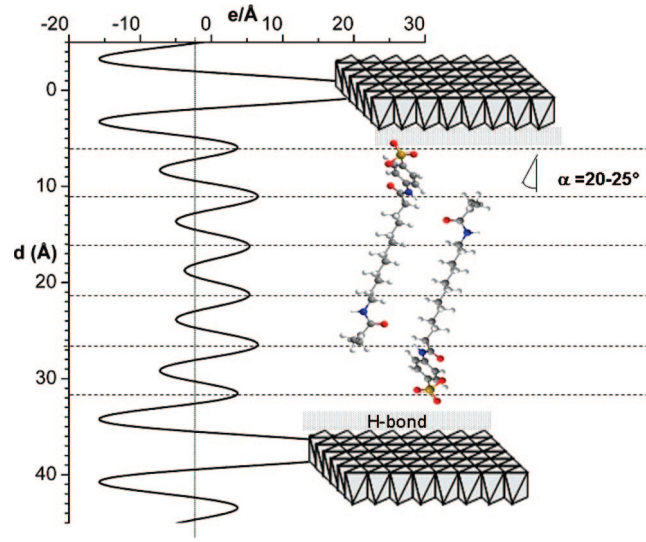

Figure 2. 1D electron density projection along the c-axis for Zn_2Al/MADABS and the corresponding structural model.

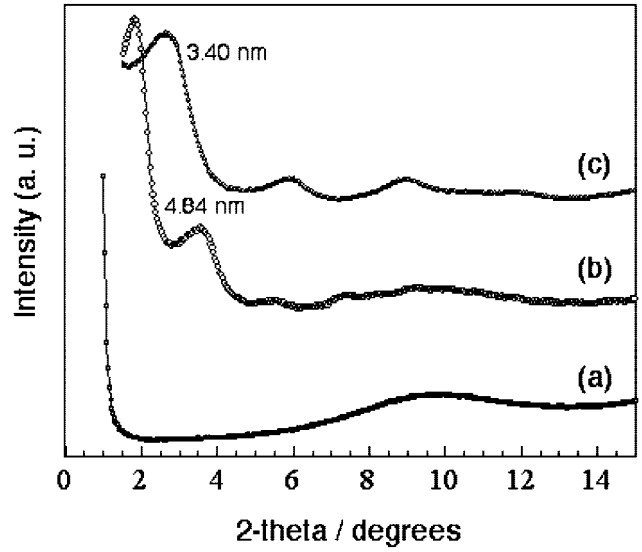

Figure 3. XRD of (1) PS and nanocomposite derivatives: nanocomposite (a) free of filler and in presence of Zn_2Al/ MADABS previously treated (c) or not (b) at 200 °C.

3.2. Zn_2Al/MADABS:PS Nanocomposite. *3.2.1. Nanocomposite Structure.* The hybrid phase Zn_2Al/MADABS is dispersed into styrene solution. After bulk polymerization, the polystyrene presents its usual amorphous state, with two large humps centered at 10° and 19° (corresponding to reticular distances of 0.46 and 0.88 nm, respectively) and attributed to some repetitive organization of PS chains (Figure 3). In the presence of the filler, intercalated PS structure is obtained, and the basal spacing is increased up to 4.84 nm.

As usual, such an increase in the stacking periodicity of the filler can be explained by the presence of PS chain between the inorganic layers, PS chains crawling within the gallery space.

(29) Pavan, P. C.; Crepaldi, E. L.; Valim, J. B. *J. Colloid Interface Sci.* **2000**, *229*, 346.
(30) Dekany, I.; Berger, F.; Imrik, K.; Lagaly, G. *Colloid Polym. Sci.* **1997**, *275*, 681.
(31) Allmann, R. *Chimia* **1970**, *24*, 99.
(32) *CS Chem3D Ultra 5.0:Ultimate Modeling, Visualization and Analysis*; CS Chem3D Ultra program; Cambridge Soft Corporation: Cambridge, 1998.

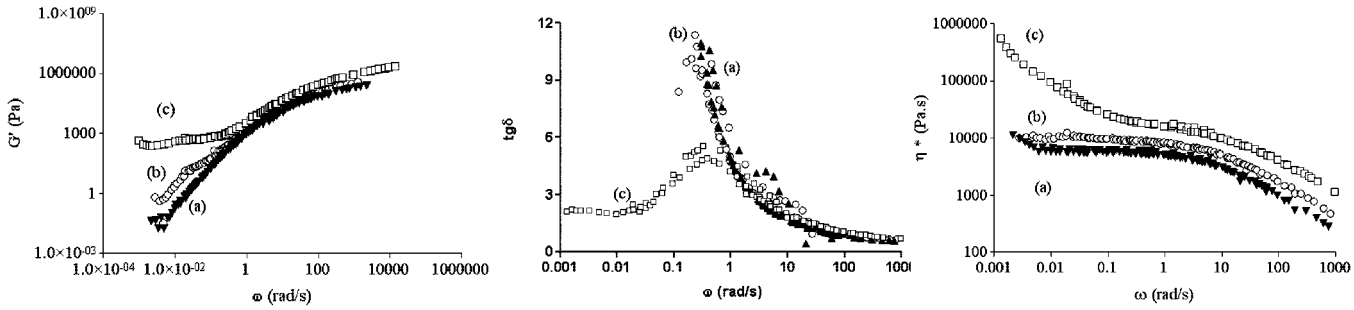

Figure 4. Master curve for (a) PS and PS nanocomposite derivatives, the filler previously treated (c) or not (b) at 200 °C, from (left) G' vs ω, (middle) tan δ vs ω, to (right) $|\eta^*|$ vs ω curves.

It was not possible to check MADABS polymerization during the PS nanocomposite film formation neither by NMR due to the strong overlap of the resonance peaks nor by FTIR because of the large number of vibration bands. Therefore, to address such a question, the hybrid phase was calcined at the temperature of the film formation, that is, 200 °C. This temperature corresponds to the upper limit of stability of Zn:Al LDH phase, above which ZnO is formed.

The crystallinity is then drastically diminished (not shown, Figure SEI 2, Supporting Information), but the basal spacing is kept constant close to its value at room temperature, that is, 3.45 nm. This may indicate that in situ polymerization has not occurred. It is worth noting the total absence of ZnO, showing the thermal stability of the hybrid phase and consistent with the enhancement in the thermal stability usually observed for the so-called organoceramic material.[33,34] Contrary to sulfopropylmethacryalte, another monomer surfactant with shorther alkyl chain,[35] the in situ polymerization of MADABS was here refuted by ^{13}CP MAS NMR analysis (Figure SEI-3, Supporting Information).

Calcined Zn_2Al/MADABS-200 material was incorporated as filler into PS. The basal spacing remained unchanged, and the expansion observed above for the uncalcined material is then not occurring for the calcined material which points out the irreversibility of the thermal process. It may be inferred that the gallery space after thermal treatment is not available for PS chain anymore to thread through its way. Yet, it is difficult to elude such a behavior owing to the absence of the in situ polymerization that would have explained the lack of lamellar expansion. The head-to-tail arrangement of MADABS molecules into the interlayer space prevents the polymerization of the acryloyl groups. Nevertheless, polymerization could take place at the particle surface wrapping the platelets and therefore hindering PS chain to crawl within the filler lamellar gap.

Consequently, it was of interest to compare both situations for which the lamellar filler is interpenetrated or not by PS chain, with MADABS tethered at the surface of the platelets either polymerizable or not, respectively.

The glass transition temperature T_g is shifted from 97 to 107 °C between PS and PS nanocomposite (not shown, Figure SEI-4, Supporting Information). Such a shift is expected in the case of polymer chain immobilization by the filler, but arrestingly, a shift of greater value (109 °C) is observed in the case of the PS "apparent immiscible" nanocomposite for which the filler is calcined prior to its dispersion.

3.2.2. Rheological Behavior. To rationalize and get more clues on the filler dispersion, rheology in the melt state was investigated. Indeed, the rheological behavior can give valuable information on the evolution of the microstructural changes over time. At first glance, one should expect an improvement of the rheological behavior from the intercalated PS structure and observe no effect or at most a deleterious one for the apparent immiscible system.

The rheological behavior of PS is well-known and presents high temperature (above T_g) features characteristic of liquid-like flow behavior with typical relaxation behaviors in the terminal zone (small ω; Figure 4a). In the low frequency domain, the elastic and loss modulus can be expressed in the power law $G' \sim \omega^2$, $G' \sim \omega^1$, respectively, and the resulting complex viscosity exhibits a plateau (Figure 4, right). The frequency dependence is slightly modified for the nanocomposite Zn_2Al/MADABS:PS, with $G' \sim \omega^{1.65}$ and $G' \sim \omega^{0.89}$, in the terminal zone, as observed on the master curve (Figure 4, left). The loss modulus is of the same amplitude (not shown), while the elastic modulus is increased by 2 orders of magnitude, giving rise to a decrease in the damping coefficient. The cross-over frequency is identical, suggesting close reptation times. The behavior is drastically modified for the other nanocomposite Zn_2Al/MADABS-200:PS, for which a nearly frequency independent feature is observed at low ω (Figure 4, left). This is even more visible from the change in the slope of the complex viscosity $|\eta^*|$ vs ω with an associated shear thinning exponent different from zero, $|\eta^*| \rightarrow \omega^{-0.55}$ (Figure 4, right). Additionally, the values of G' and G'' are largely increased, and the curve of the damping coefficient δ is strongly modified (Figure 4, middle). Furthermore, the cross-over frequency is shifted to greater times (smaller ω). Such behavior typical of solid-like flow maybe explained by an increase in the frictional interactions. The absence of terminal behavior suggests the presence of interactions between filler platelets and PS chains, restricting the plastic deformation and impeding the chain motion, and thus giving rise to a "chemical friction welding" between the components. This result is consistent with the increase in T_g. Such behavior has been observed in other systems in which the two

(33) Messersmith, P. B.; Stupp, S. I. *Chem. Mater.* **1995**, *7*, 454.
(34) Moujahid, M.; Besse, J.-P.; Leroux, F. *J. Mater. Chem.* **2003**, *13*, 258.
(35) Roland-Swanson, C.; Besse, J.-P.; Leroux, F. *Chem. Mater.* **2004**, *16*, 5512.

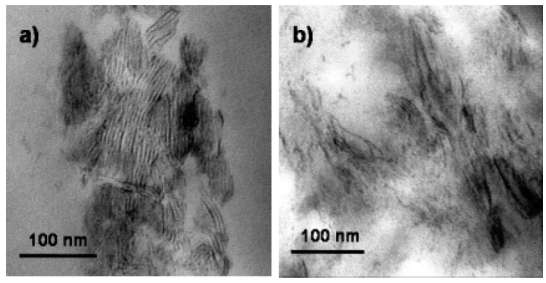

Figure 5. TEM images of PS nanocomposite with the emulsifier-modified LDH filler Zn_2Al/ MADABS previously treated (b) or not (a) at 200 °C.

components, filler and polymer, are tethered[36] or anchored[37] between each other, but it is rather unexpected for a "non-miscible" polymer nanocomposite structure.

Before going further, it is important to mention that the molecular weight M_w of PS into the different samples and measured by GPC (see Experimental Section) are rather similar. Indeed, the observed differences are not due to PS chain length but to some attrition phenomena between different components. One must remember that we are dealing with a physical jamming induced somehow by a percolated network of the nanoscopic filler. Lower filler content does decrease the observed trend toward solid-like behavior (not shown). The other interesting point is that a greater interaction should be expected from an intercalated structure since it is generally conducive to act as a barrier for PS chain to flow. In our case, an incomplete relaxation is only observed for PS "apparent nonmiscible" nanocomposite which presents no PS chain incorporation.

3.2.3. Morphology of the PS Nanocomposites. To better understand the lack of improvement for the intercalated structure, the samples were observed by TEM (Figure 5a). In spite of the organophilicity of the platelets allowing PS chains to enter within the interlayer space, as shown by XRD, and to form an expanded intercalated structure into PS, Zn_2Al/MADABS was found to agglomerate, the LDH tactoids being clustered together in large agglomerates. The lateral size of the stacked filler domain is comprised in between 50 and 100 nm, and an average of 10 platelets (from 5 up to 15) forms the aggregation resulting in a dimension from 30 up to more than 100 nm. On the contrary Zn_2Al/MADABS-200 platelets are well-dispersed although not exfoliated (Figure 5b) and form an interconnected network within the PS matrix, composed of filler domain presenting a lateral size between 50 to 100 nm, with an average of less than five platelets (<30 nm). This difference between PS nanocomposites was observed in all the observed spots by TEM and using lower magnification, showing either the aggregation of stacked PS interleaved hybrid platelets or the nonmiscible homogenously dispersed LDH tactoids.

These apparent discrepancies may be interpreted as follows. The length of the MADABS alkyl chain is suitable to prop apart the layers, but the head-to-tail

Scheme 2. Schematic Illustration Showing the Effect of the Thermal Treatment on the Filler Dispersion[a]

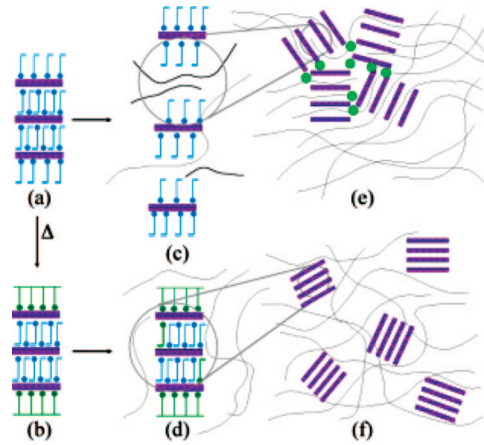

[a] (a, c, and e) For Zn_2Al/MADABS and its dispersion into PS, (b, d, and f) for Zn_2Al/MADABS-200 and its corresponding schematic dispersion adapted from the TEM observation (Figure 5).

interlayer arrangement prevents the in situ polymerization. During the bulk polymerization, the diffusion kinetic of PS chain is faster than the polymerization of MADABS present on the surface of the platelets, and PS nanocomposite structure is then intercalated (Scheme 2). For the precalcined filler, the presence of polymerized MADABS molecules at the surface of the crystallite impedes PS chain to crawl within the gallery space, but such a concatenation between inorganic platelets is found not to be strong enough to impede their dispersion when dispersed into styrene solution and submitted to bulk polymerization. Sonication followed by bulk polymerization acts as a mechanical grinding, separating the secondary particles but keeping intact the stacked primary LDH units.

4. Conclusions

In summary, the characterization by 1D electron density pictures the interleaved molecule MADABS well ensconced between LDH sheets but shows the impossibility for the molecule to polymerize itself. The strong interdigitation abates the in situ polymerization. Contrary to the prevailing idea that intercalated polymer structure means an increase in the interaction between polymer chain and filler and consequently an enhancement of the mechanical properties, we have demonstrated here that such behavior may be in conjonction with agglomerates while an opposite tendency is observed for the nonintercalated structure.

It was also shown that the XRD pattern may give a deformed picture for PS structure, highlighting the need for additional characterizations such as rheology. This is somehow in agreement with Schaefer and Justice concluding that aggregation is ubiquitous, leading to large-scale tactoids structure more disordered than thought and finding its origin in the entanglement of sheets.[16] Indeed rheology is here indicative of subtle microstructure changes and maps out the relationship between degree of dispersion and interaction, complemented by TEM direct observation.

(36) Krishnamoorti, R.; Giannelis, E. P. *Macromolecules* **1997**, *30*, 4097.
(37) Wu, J.; Haddad, T. S.; Kim, G.-M.; Mather, P. *Macromolecules* **2007**, *40*, 544.

It appeared that the nonintercalated structure may be dispersed while the intercalated one may not be, and dispersion of the filler, even incomplete, is more efficient in terms of frictional interaction than for agglomerated particles even with the PS chain crawling between the layers.

Acknowledgment. The authors thank Dr. V. Prévot (LMI) for the TEM pictures.

Supporting Information Available: XRD of thermally treated Zn_2Al/MADABS; ^{13}CP-MAS solid state NMR; DSC measurements, TG analysis, and MADABS molecular simulation (PDF). This material is available free of charge via the Internet at http://pubs.acs.org.

CM800212G